ASYMPTOTIC PERFORMANCE ANALYSIS OF ESPRIT-TYPE ALGORITHMS FOR CIRCULAR AND STRICTLY NON-CIRCULAR SOURCES WITH SPATIAL SMOOTHING

Jens Steinwandt [1], *Florian Roemer* [2], *and Martin Haardt* [1]

[1] Communications Research Laboratory, Ilmenau University of Technology, P.O. Box 100565, 98684 Ilmenau, Germany
[2] Digital Broadcasting Research Laboratory, Ilmenau University of Technology, P.O. Box 100565, 98684 Ilmenau, Germany
{jens.steinwandt, florian.roemer, martin.haardt}@tu-ilmenau.de, www.tu-ilmenau.de/crl

ABSTRACT

Spatial smoothing is a widely used preprocessing scheme to improve the performance of high-resolution parameter estimation algorithms in case of coherent signals or a small number of available snapshots. In this paper, we present a first-order performance analysis of Standard and Unitary ESPRIT as well as NC Standard and NC Unitary ESPRIT for strictly second-order (SO) non-circular (NC) sources when spatial smoothing is applied. The derived expressions are asymptotic in the effective signal-to-noise ratio (SNR), i.e., the approximations become exact for either high SNRs or a large sample size. Moreover, they are explicit in the noise realizations, i.e., only a zero-mean and finite SO moments of the noise are required. We show that both NC ESPRIT-type algorithms with spatial smoothing perform asymptotically identical in the high effective SNR. Also, for the special case of a single source, we analytically derive the optimal number of subarrays for spatial smoothing and show that no gain from strictly non-circular sources is achieved in this case.

Index Terms— Performance analysis, spatial smoothing, ESPRIT, non-circular sources, DOA estimation.

1. INTRODUCTION AND STATE OF THE ART

ESPRIT-type parameter estimation algorithms [1], [2] have attracted considerable attention in a broad variety of applications such as radar, sonar, and wireless communications, due to their fully algebraic estimates and their low complexity. With the growing popularity of parameter estimation algorithms, their analytical performance analyses have been of great research interest. The two most prominent concepts are [3] and [4]. The approach in [3] analyzes the eigenvector distribution of the sample covariance matrix. It requires Gaussianity assumptions on the source symbols and the noise, and is only asymptotic in the sample size. In contrast, [4] provides a first-order approximation of the estimation error caused by the perturbed subspace estimate due to a small noise contribution. Hence, it is asymptotic in the effective signal-to-noise ratio (SNR), i.e., the results become accurate for either high SNRs or a large sample size. Therefore, [4] even applies to the case of a single snapshot if the SNR is sufficiently high. In [5]-[7], this work was extended to multi-dimensional (R-D) parameter estimation, where the derived MSE expressions only require the noise to be zero-mean with finite second-order (SO) moments.

Recently, a number of improved subspace-based parameter estimation schemes, e.g., NC MUSIC [8], NC Root-MUSIC [9], NC standard ESPRIT [10], and NC Unitary ESPRIT [11] have been developed that exploit prior knowledge about the source signals if they are strictly SO non-circular (NC) [12]. Examples include BPSK, PAM, and ASK-modulated signals. The performance of these algorithms has been investigated in [8] and [13]-[16].

The aforementioned NC and non-NC methods are known to yield a high resolution even in the case of correlated sources. However, they encounter difficulties when the signals are coherent. Assuming a uniform linear array (ULA), spatial smoothing [17]-[19] can be applied to circumvent these problems by averaging the data received by L subarrays. The resulting estimation error depends on the choice of the design parameter L. Performance assessments of spatial smoothing based on [3], which requires a large sample size, have been conducted in [20]-[22]. However, expressions for Standard and Unitary ESPRIT with spatial smoothing as well as for NC Standard and NC Unitary ESPRIT with spatial smoothing based on [4], which only requires a high effective SNR, have not been reported in the literature.

In this paper, we further extend [5] and [15] and present a performance analysis for the spatially smoothed versions of 1-D Standard and Unitary ESPRIT as well as 1-D NC Standard and NC Unitary ESPRIT assuming a ULA. The shift invariance equations are solved using least squares (LS). We derive the first-order expansions of the estimation errors that are explicit in the noise realization, and MSE expressions, where only a zero mean and finite SO moments of the noise are required. Thus, no assumptions about the noise statistics are needed. We show that both NC ESPRIT-type algorithms have the same asymptotic performance in the high effective SNR, while NC Unitary ESPRIT performs better at low effective SNRs. Further insights into the dependence of the MSE on the physical parameters are provided by the case study of a single source. For this case, we analytically find the optimal number of subarrays L for the spatial smoothing and show that no gain from strictly non-circular sources is obtained.

2. DATA MODEL

2.1. General Model

Assume that a ULA consisting of M isotropic elements receives narrowband signals from d far-field sources. The N subsequent data observations can be modeled as

$$\boldsymbol{X} = \boldsymbol{A}\boldsymbol{S} + \boldsymbol{N} = \boldsymbol{X}_0 + \boldsymbol{N} \in \mathbb{C}^{M\times N}, \tag{1}$$

where $\boldsymbol{A} = [\boldsymbol{a}(\mu_1), \ldots, \boldsymbol{a}(\mu_d)] \in \mathbb{C}^{M\times d}$ is the array steering matrix, which contains the array steering vectors $\boldsymbol{a}(\mu_i)$ corresponding to the i-th spatial frequency μ_i with $i = 1, \ldots, d$. The matrix $\boldsymbol{S} \in \mathbb{C}^{d\times N}$ represents the source symbol matrix, and $\boldsymbol{N} \in \mathbb{C}^{M\times N}$ consists of the additive sensor noise samples. As we apply ESPRIT-type algorithms using a ULA to estimate the parameters, the shift invariance $\boldsymbol{J}_1\boldsymbol{A}\boldsymbol{\Phi} = \boldsymbol{J}_2\boldsymbol{A}$ holds, where $\boldsymbol{J}_1$ and $\boldsymbol{J}_2 \in \mathbb{R}^{(M-1)\times M}$ are

This work was supported by the International Graduate School on Mobile Communications (MOBICOM), Ilmenau, Germany.

the selection matrices for the first and the second subarray with maximum overlap, and $\boldsymbol{\Phi} = \mathrm{diag}\{[e^{\mathrm{j}\mu_1}, \ldots, e^{\mathrm{j}\mu_d}]\} \in \mathbb{C}^{d\times d}$ contains the spatial frequencies to be estimated [2]. Based on (1), the signal subspace $\hat{\boldsymbol{U}}_\mathrm{s} \in \mathbb{C}^{M\times d}$ is estimated by computing the d dominant left singular vectors of $\boldsymbol{X}$. As $\boldsymbol{A}$ and $\hat{\boldsymbol{U}}_\mathrm{s}$ span approximately the same column space, a non-singular matrix $\boldsymbol{T} \in \mathbb{C}^{d\times d}$ can be found such that $\boldsymbol{A} \approx \hat{\boldsymbol{U}}_\mathrm{s}\boldsymbol{T}$. Then, the shift invariance equation can be expressed in terms of the estimated signal subspace, yielding $\boldsymbol{J}_1\hat{\boldsymbol{U}}_\mathrm{s}\boldsymbol{\Upsilon} \approx \boldsymbol{J}_2\hat{\boldsymbol{U}}_\mathrm{s}$ with $\boldsymbol{\Upsilon} \approx \boldsymbol{T}\boldsymbol{\Phi}\boldsymbol{T}^{-1}$. Often, the unknown matrix $\boldsymbol{\Upsilon}$ is estimated using least squares (LS), i.e., $\hat{\boldsymbol{\Upsilon}} = (\boldsymbol{J}_1\hat{\boldsymbol{U}}_\mathrm{s})^{+}\boldsymbol{J}_2\hat{\boldsymbol{U}}_\mathrm{s} \in \mathbb{C}^{d\times d}$, where $^{+}$ stands for the Moore-Penrose pseudo inverse. Finally, the spatial frequency estimates are obtained by $\hat{\mu}_i = \arg\{\hat{\lambda}_i\},\ i = 1, \ldots, d$, where $\hat{\lambda}_i$ are the eigenvalues of $\hat{\boldsymbol{\Upsilon}}$.

If some of the received signals are coherent, i.e., fully correlated, the symbol matrix $\boldsymbol{S}$ is singular and therefore rank deficient. Consequently, the directions of the coherent signals cannot be estimated. In this case, spatial smoothing can be applied as a preprocessing scheme that restores the full row rank d of $\boldsymbol{S}$ albeit reducing the effective array aperture. To this end, the ULA with M sensors is divided into L maximally overlapping subarrays, each containing $M_\mathrm{sub} = M - L + 1$ sensor elements. Let the selection matrix that corresponds to the ℓ-th subarray, $1 \le \ell \le L$, be defined as

$$\boldsymbol{J}_\ell^{(M)} = [\boldsymbol{0}_{M_\mathrm{sub}\times(\ell-1)}\ \ \boldsymbol{I}_{M_\mathrm{sub}}\ \ \boldsymbol{0}_{M_\mathrm{sub}\times(L-\ell)}] \in \mathbb{R}^{M_\mathrm{sub}\times M}. \quad (2)$$

The spatially smoothed data matrix $\boldsymbol{X}_\mathrm{SS}$, which is subsequently processed instead of $\boldsymbol{X}$, is given by

$$\begin{aligned}\boldsymbol{X}_\mathrm{SS} &= \left[\boldsymbol{J}_1^{(M)}\boldsymbol{X} \quad \boldsymbol{J}_2^{(M)}\boldsymbol{X} \quad \cdots \quad \boldsymbol{J}_L^{(M)}\boldsymbol{X}\right] \in \mathbb{C}^{M_\mathrm{sub}\times NL} \\ &= \boldsymbol{X}_{0\mathrm{SS}} + \boldsymbol{N}_\mathrm{SS}, \end{aligned} \quad (3)$$

where $\boldsymbol{X}_{0\mathrm{SS}}$ is the noise-free spatially smoothed data matrix. Note that we require $\min\{M - L, NL\} \ge d$ to estimate the d spatial frequencies.

2.2. Strictly Non-Circular Sources

In the case of strictly SO non-circular sources, the complex symbol amplitudes of each source lie on a rotated line in the complex plane. Therefore, $\boldsymbol{S}$ can be written as $\boldsymbol{S} = \boldsymbol{\Psi}\boldsymbol{S}_0$, where $\boldsymbol{S}_0 \in \mathbb{R}^{d\times N}$ is a real-valued symbol matrix and $\boldsymbol{\Psi} = \mathrm{diag}\{e^{\mathrm{j}\varphi_i}\}_{i=1}^{d}$ contains complex phase shifts on its diagonal that can be different for each received signal [11]. In order to take advantage of this property, we apply a preprocessing scheme to (1) and define the augmented measurement matrix $\boldsymbol{X}^{(\mathrm{nc})} \in \mathbb{C}^{2M\times N}$ as [11]

$$\boldsymbol{X}^{(\mathrm{nc})} = \begin{bmatrix}\boldsymbol{X} \\ \boldsymbol{\Pi}_M\boldsymbol{X}^*\end{bmatrix} = \boldsymbol{A}^{(\mathrm{nc})}\boldsymbol{S} + \boldsymbol{N}^{(\mathrm{nc})} = \boldsymbol{X}_0^{(\mathrm{nc})} + \boldsymbol{N}^{(\mathrm{nc})}, \quad (4)$$

where $\boldsymbol{\Pi}_M$ is the $M \times M$ exchange matrix with ones on its antidiagonal and zeros elsewhere. Applying a modified spatial smoothing concept to (4) [11], we select $2M_\mathrm{sub}$ out of $2M$ virtual sensors. Thus, the selection matrices (2) are extended to $\boldsymbol{J}_\ell^{(M)(\mathrm{nc})} = \boldsymbol{I}_2 \otimes \boldsymbol{J}_\ell^{(M)} \in \mathbb{R}^{2M_\mathrm{sub}\times 2M}$. The resulting spatially smoothed data matrix of size $2M_\mathrm{sub} \times NL$ is then given by

$$\begin{aligned}\boldsymbol{X}_\mathrm{SS}^{(\mathrm{nc})} &= \left[\boldsymbol{J}_1^{(M)(\mathrm{nc})}\boldsymbol{X}^{(\mathrm{nc})} \quad \cdots \quad \boldsymbol{J}_L^{(M)(\mathrm{nc})}\boldsymbol{X}^{(\mathrm{nc})}\right] \\ &= \boldsymbol{X}_{0_\mathrm{SS}}^{(\mathrm{nc})} + \boldsymbol{N}_\mathrm{SS}^{(\mathrm{nc})}, \end{aligned} \quad (5)$$

where $\boldsymbol{X}_{0_\mathrm{SS}}^{(\mathrm{nc})}$ is the unperturbed spatially smoothed NC data matrix. Note that spatial smoothing cannot be applied before $\boldsymbol{X}^{(\mathrm{nc})}$ is formed (4) as this would destroy the structure of the source signals.

3. PERFORMANCE OF ESPRIT-TYPE ALGORITHMS WITH SPATIAL SMOOTHING

In this section, we derive first-order error expansions of Standard ESPRIT and Unitary ESPRIT both with spatial smoothing. Our expressions rely on the data model (3) in Section 2.1.

3.1. Standard ESPRIT with Spatial Smoothing

For the perturbation analysis of the estimation error, we adopt the analytical framework proposed in [4] and [5]. Therein, an explicit first-order error expansion is derived assuming that the additive noise perturbation is small and zero-mean with finite SO moments. These assumptions are not violated by the spatial smoothing preprocessing such that [4] and [5] can be used for the presented development.

To derive the signal subspace estimation error for (3), we express the SVD of the noise-free spatially smoothed observations $\boldsymbol{X}_{0\mathrm{SS}}$ as

$$\boldsymbol{X}_{0\mathrm{SS}} = \begin{bmatrix}\boldsymbol{U}_{\mathrm{SS_s}} & \boldsymbol{U}_{\mathrm{SS_n}}\end{bmatrix}\begin{bmatrix}\boldsymbol{\Sigma}_{\mathrm{SS_s}} & \boldsymbol{0} \\ \boldsymbol{0} & \boldsymbol{0}\end{bmatrix}\begin{bmatrix}\boldsymbol{V}_{\mathrm{SS_s}} & \boldsymbol{V}_{\mathrm{SS_n}}\end{bmatrix}^{\mathrm{H}}, \quad (6)$$

where $\boldsymbol{U}_{\mathrm{SS_s}} \in \mathbb{C}^{M_\mathrm{sub}\times d}$, $\boldsymbol{U}_{\mathrm{SS_n}} \in \mathbb{C}^{M_\mathrm{sub}\times(NL-d)}$, as well as $\boldsymbol{V}_{\mathrm{SS_s}} \in \mathbb{C}^{NL\times d}$ span the signal subspace, the noise subspace, and the row space respectively, and $\boldsymbol{\Sigma}_{\mathrm{SS_s}} \in \mathbb{R}^{d\times d}$ contains the non-zero singular values on its diagonal. Writing the perturbed signal subspace estimate $\hat{\boldsymbol{U}}_{\mathrm{SS_s}}$ as $\hat{\boldsymbol{U}}_{\mathrm{SS_s}} = \boldsymbol{U}_{\mathrm{SS_s}} + \Delta\boldsymbol{U}_{\mathrm{SS_s}}$, where $\Delta\boldsymbol{U}_{\mathrm{SS_s}}$ denotes the signal subspace error, we get the first-order approximation [4]

$$\Delta\boldsymbol{U}_{\mathrm{SS_s}} = \boldsymbol{U}_{\mathrm{SS_n}}\boldsymbol{U}_{\mathrm{SS_n}}^{\mathrm{H}}\boldsymbol{N}_\mathrm{SS}\boldsymbol{V}_{\mathrm{SS_s}}\boldsymbol{\Sigma}_{\mathrm{SS_s}}^{-1} + \mathcal{O}\{\Delta^2\}, \quad (7)$$

where $\Delta = \|\boldsymbol{N}_\mathrm{SS}\|$, and $\|\cdot\|$ represents a submultiplicative norm. For the estimation error of the i-th spatial frequency obtained by the LS solution, we have [4]

$$\begin{aligned}\Delta\mu_i = \mathrm{Im}\Big\{\boldsymbol{p}_i^{\mathrm{T}}\,(\boldsymbol{J}_{\mathrm{SS}1}\boldsymbol{U}_{\mathrm{SS_s}})^{+}\,[\boldsymbol{J}_{\mathrm{SS}2}/\lambda_i \\ -\boldsymbol{J}_{\mathrm{SS}1}]\,\Delta\boldsymbol{U}_{\mathrm{SS_s}}\boldsymbol{q}_i\Big\} + \mathcal{O}\{\Delta^2\},\end{aligned} \quad (8)$$

where $\lambda_i = e^{\mathrm{j}\mu_i}$ is the i-th eigenvalue of $\boldsymbol{\Upsilon}$, $\boldsymbol{q}_i$ represents the i-th eigenvector of $\boldsymbol{\Upsilon}$ and the i-th column vector of the eigenvector matrix $\boldsymbol{Q}$, and $\boldsymbol{p}_i^{\mathrm{T}}$ is the i-th row vector of $\boldsymbol{P} = \boldsymbol{Q}^{-1}$. Hence, the eigendecomposition of $\boldsymbol{\Upsilon}$ is given by $\boldsymbol{\Upsilon} = \boldsymbol{Q}\boldsymbol{\Lambda}\boldsymbol{Q}^{-1}$, where $\boldsymbol{\Lambda}$ contains the eigenvalues λ_i on its diagonal. Moreover, $\boldsymbol{J}_{\mathrm{SS}1}$ and $\boldsymbol{J}_{\mathrm{SS}2}$ select the subarrays with $M - L$ out of M_sub sensors.

Finally, to compute the MSE expression for Standard ESPRIT with spatial smoothing, we extend the results in [5]. The MSE for the i-th spatial frequency is given by

$$\begin{aligned}\mathbb{E}\left\{(\Delta\mu_i)^2\right\} = \frac{1}{2}\Big(\boldsymbol{r}_{\mathrm{SS}i}{}^{\mathrm{H}}\boldsymbol{W}_\mathrm{SS}^{*}\boldsymbol{R}_\mathrm{SS}^{\mathrm{T}}\boldsymbol{W}_\mathrm{SS}^{\mathrm{T}}\boldsymbol{r}_{\mathrm{SS}i} \\ -\mathrm{Re}\Big\{\boldsymbol{r}_{\mathrm{SS}i}{}^{\mathrm{T}}\boldsymbol{W}_\mathrm{SS}\boldsymbol{C}_\mathrm{SS}^{\mathrm{T}}\boldsymbol{W}_\mathrm{SS}^{\mathrm{T}}\boldsymbol{r}_{\mathrm{SS}i}\Big\}\Big) + \mathcal{O}\{\Delta^2\},\end{aligned} \quad (9)$$

where

$$\boldsymbol{r}_{\mathrm{SS}i} = \boldsymbol{q}_i \otimes \left(\left[(\boldsymbol{J}_{\mathrm{SS}1}\boldsymbol{U}_{\mathrm{SS_s}})^{+}\,(\boldsymbol{J}_{\mathrm{SS}2}/\lambda_i - \boldsymbol{J}_{\mathrm{SS}1})\right]^{\mathrm{T}}\boldsymbol{p}_i\right),$$

$$\boldsymbol{W}_\mathrm{SS} = \left(\boldsymbol{\Sigma}_{\mathrm{SS_s}}{}^{-1}\boldsymbol{V}_{\mathrm{SS_s}}{}^{\mathrm{T}}\right) \otimes \left(\boldsymbol{U}_{\mathrm{SS_n}}\boldsymbol{U}_{\mathrm{SS_n}}{}^{\mathrm{H}}\right).$$

Next, we derive the covariance matrix $\boldsymbol{R}_\mathrm{SS} = \mathbb{E}\{\boldsymbol{n}_\mathrm{SS}\boldsymbol{n}_\mathrm{SS}^{\mathrm{H}}\}$ and the pseudo-covariance matrix $\boldsymbol{C}_\mathrm{SS} = \mathbb{E}\{\boldsymbol{n}_\mathrm{SS}\boldsymbol{n}_\mathrm{SS}^{\mathrm{T}}\}$ of the spatially smoothed noise $\boldsymbol{n}_\mathrm{SS} = \mathrm{vec}\{\boldsymbol{N}_\mathrm{SS}\} \in \mathbb{C}^{M_\mathrm{sub}NL\times 1}$ needed for (9). Applying the vec-operator to $\boldsymbol{N}_\mathrm{SS}$ in (3) and using the property $\mathrm{vec}\{\boldsymbol{A}\boldsymbol{X}\boldsymbol{B}\} = (\boldsymbol{B}^{\mathrm{T}} \otimes \boldsymbol{A}) \cdot \mathrm{vec}\{\boldsymbol{X}\}$ for arbitrary matrices $\boldsymbol{A}$, $\boldsymbol{B}$, and $\boldsymbol{X}$ of appropriate sizes, we obtain

$$\boldsymbol{n}_\mathrm{SS} = \boldsymbol{Q} \cdot \boldsymbol{n}, \quad (10)$$

where $\boldsymbol{Q} = [(\boldsymbol{I}_N \otimes \boldsymbol{J}_1^{(M)})^{\mathrm{T}}, \cdots, (\boldsymbol{I}_N \otimes \boldsymbol{J}_L^{(M)})^{\mathrm{T}}]^{\mathrm{T}} \in \mathbb{R}^{M_{\mathrm{sub}}NL \times MN}$ and $\boldsymbol{n} = \mathrm{vec}\{\boldsymbol{N}\} \in \mathbb{C}^{MN \times 1}$. Thus, the SO statistics of $\boldsymbol{n}_{\mathrm{SS}}$ can be expressed in terms of the covariance matrix $\boldsymbol{R}_{\mathrm{nn}} = \mathbb{E}\{\boldsymbol{n}\boldsymbol{n}^{\mathrm{H}}\}$ and the pseudo-covariance matrix $\boldsymbol{C}_{\mathrm{nn}} = \mathbb{E}\{\boldsymbol{n}\boldsymbol{n}^{\mathrm{T}}\}$ of the unsmoothed noise component $\boldsymbol{n}$, i.e.,

$$\boldsymbol{R}_{\mathrm{SS}} = \mathrm{blkdiag}\{\boldsymbol{Q}\}\,(\boldsymbol{1}_L \otimes \boldsymbol{R}_{\mathrm{nn}})\,\mathrm{blkdiag}\{\boldsymbol{Q}\}^{\mathrm{H}}, \tag{11}$$

$$\boldsymbol{C}_{\mathrm{SS}} = \mathrm{blkdiag}\{\boldsymbol{Q}\}\,(\boldsymbol{1}_L \otimes \boldsymbol{C}_{\mathrm{nn}})\,\mathrm{blkdiag}\{\boldsymbol{Q}\}^{\mathrm{H}}, \tag{12}$$

where $\boldsymbol{1}_L$ is the $L \times L$ matrix of ones and $\mathrm{blkdiag}\{\boldsymbol{Q}\}$ places the blocks of $\boldsymbol{Q}$ on the block diagonal.

3.2. Unitary ESPRIT with Spatial Smoothing

It was shown in [5] that the asymptotic performance of Unitary-ESPRIT-type algorithms is found once forward-backward-averaging (FBA) is taken into account. FBA is performed by replacing the spatially smoothed data matrix $\boldsymbol{X}_{\mathrm{SS}} \in \mathbb{C}^{M_{\mathrm{sub}} \times NL}$ by the column-augmented data matrix $\tilde{\boldsymbol{X}}_{\mathrm{SS}} \in \mathbb{C}^{M_{\mathrm{sub}} \times 2NL}$ defined by

$$\tilde{\boldsymbol{X}}_{\mathrm{SS}} = \begin{bmatrix}\boldsymbol{X}_{\mathrm{SS}} & \boldsymbol{\Pi}_{2M}\boldsymbol{X}_{\mathrm{SS}}^{*}\boldsymbol{\Pi}_{N}\end{bmatrix} = \tilde{\boldsymbol{X}}_{0\mathrm{SS}} + \tilde{\boldsymbol{N}}_{\mathrm{SS}}, \tag{13}$$

where $\tilde{\boldsymbol{X}}_{0\mathrm{SS}}$ is the noiseless FBA-processed spatially smoothed data matrix. The transformation (13) does not alter the assumptions made in the previous subsection. Hence, the same performance analysis framework is applicable to (13). We replace the noise-free subspaces of $\boldsymbol{X}_{0\mathrm{SS}}$ in (8) by the corresponding subspaces of $\tilde{\boldsymbol{X}}_{0\mathrm{SS}}$, and $\boldsymbol{p}_i$ and $\boldsymbol{q}_i$ by $\tilde{\boldsymbol{p}}_i$ and $\tilde{\boldsymbol{q}}_i$, respectively, to obtain

$$\begin{aligned}\Delta\mu_i = \mathrm{Im}\Big\{\tilde{\boldsymbol{p}}_i^{\mathrm{T}}\left(\boldsymbol{J}_{\mathrm{SS}1}\tilde{\boldsymbol{U}}_{\mathrm{SS_s}}\right)^{+}[\boldsymbol{J}_{\mathrm{SS}2}/\lambda_i \\ -\boldsymbol{J}_{\mathrm{SS}1}]\,\Delta\tilde{\boldsymbol{U}}_{\mathrm{SS_s}}\tilde{\boldsymbol{q}}_i\Big\} + \mathcal{O}\{\Delta^2\},\end{aligned} \tag{14}$$

where the signal subspace error $\Delta\tilde{\boldsymbol{U}}_{\mathrm{SS_s}} \in \mathbb{C}^{M_{\mathrm{sub}} \times d}$ is given by

$$\Delta\tilde{\boldsymbol{U}}_{\mathrm{SS_s}} = \tilde{\boldsymbol{U}}_{\mathrm{SS_n}}\tilde{\boldsymbol{U}}_{\mathrm{SS_n}}^{\mathrm{H}}\tilde{\boldsymbol{N}}_{\mathrm{SS}}\tilde{\boldsymbol{V}}_{\mathrm{SS_s}}\tilde{\boldsymbol{\Sigma}}_{\mathrm{SS_s}}^{-1} + \mathcal{O}\{\Delta^2\}. \tag{15}$$

Similarly, expression (9) can be applied to compute the MSE for Unitary ESPRIT with spatial smoothing by replacing all quantities with their forward-backward-averaged equivalents. It can be shown that $\tilde{\boldsymbol{n}}_{\mathrm{SS}} = \mathrm{vec}\{\tilde{\boldsymbol{N}}_{\mathrm{SS}}\} \in \mathbb{C}^{2M_{\mathrm{sub}}NL \times 1}$ is given by

$$\tilde{\boldsymbol{n}}_{\mathrm{SS}} = \begin{bmatrix}\boldsymbol{n}_{\mathrm{SS}}^{\mathrm{T}} & (\boldsymbol{\Pi}_{M_{\mathrm{sub}}NL}\boldsymbol{n}_{\mathrm{SS}}^{*})^{\mathrm{T}}\end{bmatrix}^{\mathrm{T}}. \tag{16}$$

Therefore, the expressions for $\tilde{\boldsymbol{R}}_{\mathrm{SS}} = \mathbb{E}\{\tilde{\boldsymbol{n}}_{\mathrm{SS}}\tilde{\boldsymbol{n}}_{\mathrm{SS}}^{\mathrm{H}}\}$ and $\tilde{\boldsymbol{C}}_{\mathrm{SS}} = \mathbb{E}\{\tilde{\boldsymbol{n}}_{\mathrm{SS}}\tilde{\boldsymbol{n}}_{\mathrm{SS}}^{\mathrm{T}}\}$ can be derived in terms of (11) and (12) as

$$\tilde{\boldsymbol{R}}_{\mathrm{SS}} = \boldsymbol{P}\begin{bmatrix}\boldsymbol{R}_{\mathrm{SS}} & \boldsymbol{C}_{\mathrm{SS}} \\ \boldsymbol{C}_{\mathrm{SS}}^{*} & \boldsymbol{R}_{\mathrm{SS}}^{*}\end{bmatrix}\boldsymbol{P}^{\mathrm{H}},\ \tilde{\boldsymbol{C}}_{\mathrm{SS}} = \boldsymbol{P}\begin{bmatrix}\boldsymbol{C}_{\mathrm{SS}} & \boldsymbol{R}_{\mathrm{SS}} \\ \boldsymbol{R}_{\mathrm{SS}}^{*} & \boldsymbol{C}_{\mathrm{SS}}^{*}\end{bmatrix}\boldsymbol{P}^{\mathrm{H}},$$

where $\boldsymbol{P} = \mathrm{blkdiag}\{\boldsymbol{I}_{M_{\mathrm{sub}}NL},\ \boldsymbol{\Pi}_{M_{\mathrm{sub}}NL}\}$.

4. PERFORMANCE OF NC ESPRIT-TYPE ALGORITHMS WITH SPATIAL SMOOTHING

In this section, we derive first-order error approximations of NC Standard ESPRIT and NC Unitary ESPRIT both with spatial smoothing for strictly non-circular sources. Our results are based on the data model (5) in Section 2.2.

4.1. NC Standard ESPRIT with Spatial Smoothing

In [15], we have observed that the preprocessing scheme for non-circular sources does not affect the assumptions of a small noise perturbation with zero-mean and finite SO moments. As a consequence, the framework of [4] is applicable to the augmented measurement matrix $\boldsymbol{X}^{(\mathrm{nc})}$ given in (4). From the model (5), it is apparent that adding spatial smoothing as a second preprocessing step does not violate these assumptions either, which is also consistent with the reasoning in Section 3.1. Therefore, the same procedure as in Section 3.1 can be applied to the spatially smoothed augmented data matrix $\boldsymbol{X}_{\mathrm{SS}}^{(\mathrm{nc})}$.

We are first interested in the perturbation of the subspace of the matrix $\boldsymbol{X}_{0_{\mathrm{SS}}}^{(\mathrm{nc})}$ superimposed by the small additive perturbation $\boldsymbol{N}_{\mathrm{SS}}^{(\mathrm{nc})}$. Extracting the noise-free subspaces from the SVD of $\boldsymbol{X}_{0_{\mathrm{SS}}}^{(\mathrm{nc})}$ similarly to (6), we obtain [4]

$$\Delta\boldsymbol{U}_{\mathrm{SS_s}}^{(\mathrm{nc})} = \boldsymbol{U}_{\mathrm{SS_n}}^{(\mathrm{nc})}\boldsymbol{U}_{\mathrm{SS_n}}^{(\mathrm{nc})^{\mathrm{H}}}\boldsymbol{N}_{\mathrm{SS}}^{(\mathrm{nc})}\boldsymbol{V}_{\mathrm{SS_s}}^{(\mathrm{nc})}\boldsymbol{\Sigma}_{\mathrm{SS_s}}^{(\mathrm{nc})^{-1}} + \mathcal{O}\{\Delta^2\}. \tag{17}$$

Then, correspondingly to (8), the estimation error of NC Standard ESPRIT with spatial smoothing can be written as

$$\begin{aligned}\Delta\mu_i = \mathrm{Im}\Big\{\boldsymbol{p}_i^{(\mathrm{nc})^{\mathrm{T}}}\left(\boldsymbol{J}_{\mathrm{SS}_1}^{(\mathrm{nc})}\boldsymbol{U}_{\mathrm{SS_s}}^{(\mathrm{nc})}\right)^{+}\Big[\boldsymbol{J}_{\mathrm{SS}_2}^{(\mathrm{nc})}/\lambda_i \\ -\boldsymbol{J}_{\mathrm{SS}_1}^{(\mathrm{nc})}\Big]\,\Delta\boldsymbol{U}_{\mathrm{SS_s}}^{(\mathrm{nc})}\boldsymbol{q}_i^{(\mathrm{nc})}\Big\} + \mathcal{O}\{\Delta^2\},\end{aligned} \tag{18}$$

where $\boldsymbol{p}_i^{(\mathrm{nc})}$ and $\boldsymbol{q}_i^{(\mathrm{nc})}$ replace $\boldsymbol{p}_i$ and $\boldsymbol{q}_i$ respectively, and the NC selection matrices $\boldsymbol{J}_{\mathrm{SS}_n}^{(\mathrm{nc})}, n = 1, 2$, are given by $\boldsymbol{J}_{\mathrm{SS}_n}^{(\mathrm{nc})} = \boldsymbol{I}_2 \otimes \boldsymbol{J}_{\mathrm{SS}\,n}$ for a ULA.

For the MSE, we again apply the expression (9) and replace the corresponding quantities. The spatially smoothed augmented noise contribution $\boldsymbol{n}_{\mathrm{SS}}^{(\mathrm{nc})} = \mathrm{vec}\{\boldsymbol{N}_{\mathrm{SS}}^{(\mathrm{nc})}\} \in \mathbb{C}^{2M_{\mathrm{sub}}NL \times 1}$ can be expressed as

$$\boldsymbol{n}_{\mathrm{SS}}^{(\mathrm{nc})} = \boldsymbol{Q}^{(\mathrm{nc})} \cdot \boldsymbol{n}^{(\mathrm{nc})}, \tag{19}$$

where $\boldsymbol{Q}^{(\mathrm{nc})} = [(\boldsymbol{I}_N \otimes \boldsymbol{J}_1^{(M)(\mathrm{nc})})^{\mathrm{T}}, \cdots, (\boldsymbol{I}_N \otimes \boldsymbol{J}_L^{(M)(\mathrm{nc})})^{\mathrm{T}}]^{\mathrm{T}} \in \mathbb{R}^{2M_{\mathrm{sub}}NL \times 2MN}$ and $\boldsymbol{n}^{(\mathrm{nc})} = \tilde{\boldsymbol{K}} \cdot [\boldsymbol{n}^{\mathrm{T}}, \boldsymbol{n}^{\mathrm{H}}]^{\mathrm{T}} \in \mathbb{C}^{2MN \times 1}$ with $\tilde{\boldsymbol{K}} = \boldsymbol{K}_{2M,N}^{\mathrm{T}} \cdot \mathrm{blkdiag}\{\boldsymbol{K}_{M,N}, \boldsymbol{K}_{M,N} \cdot (\boldsymbol{I}_{NL} \otimes \boldsymbol{\Pi}_{M_{\mathrm{sub}}})\}$ [15]. The commutation matrix $\boldsymbol{K}_{M,N} \in \mathbb{R}^{MN \times MN}$ is the matrix that satisfies $\boldsymbol{K}_{M,N} \cdot \mathrm{vec}\{\boldsymbol{A}\} = \mathrm{vec}\{\boldsymbol{A}^{\mathrm{T}}\}$ for arbitrary matrices $\boldsymbol{A} \in \mathbb{C}^{M \times N}$ [23]. Then, $\boldsymbol{R}_{\mathrm{SS}}^{(\mathrm{nc})} = \mathbb{E}\{\boldsymbol{n}_{\mathrm{SS}}^{(\mathrm{nc})}\boldsymbol{n}_{\mathrm{SS}}^{(\mathrm{nc})^{\mathrm{H}}}\}$ and $\boldsymbol{C}_{\mathrm{SS}}^{(\mathrm{nc})} = \mathbb{E}\{\boldsymbol{n}_{\mathrm{SS}}^{(\mathrm{nc})}\boldsymbol{n}_{\mathrm{SS}}^{(\mathrm{nc})^{\mathrm{T}}}\}$ can be computed as

$$\boldsymbol{R}_{\mathrm{SS}}^{(\mathrm{nc})} = \mathrm{blkdiag}\big\{\boldsymbol{Q}^{(\mathrm{nc})}\big\}\Big(\boldsymbol{1}_L \otimes \boldsymbol{R}_{\mathrm{nn}}^{(\mathrm{nc})}\Big)\mathrm{blkdiag}\big\{\boldsymbol{Q}^{(\mathrm{nc})}\big\}^{\mathrm{H}},$$

$$\boldsymbol{C}_{\mathrm{SS}}^{(\mathrm{nc})} = \mathrm{blkdiag}\big\{\boldsymbol{Q}^{(\mathrm{nc})}\big\}\Big(\boldsymbol{1}_L \otimes \boldsymbol{C}_{\mathrm{nn}}^{(\mathrm{nc})}\Big)\mathrm{blkdiag}\big\{\boldsymbol{Q}^{(\mathrm{nc})}\big\}^{\mathrm{H}},$$

where $\boldsymbol{R}_{\mathrm{nn}}^{(\mathrm{nc})} = \mathbb{E}\{\boldsymbol{n}^{(\mathrm{nc})}\boldsymbol{n}^{(\mathrm{nc})^{\mathrm{H}}}\}$ and $\boldsymbol{C}_{\mathrm{nn}}^{(\mathrm{nc})} = \mathbb{E}\{\boldsymbol{n}^{(\mathrm{nc})}\boldsymbol{n}^{(\mathrm{nc})^{\mathrm{T}}}\}$ are given by [15]

$$\boldsymbol{R}_{\mathrm{nn}}^{(\mathrm{nc})} = \tilde{\boldsymbol{K}}\begin{bmatrix}\boldsymbol{R}_{\mathrm{nn}} & \boldsymbol{C}_{\mathrm{nn}} \\ \boldsymbol{C}_{\mathrm{nn}}^{*} & \boldsymbol{R}_{\mathrm{nn}}^{*}\end{bmatrix}\tilde{\boldsymbol{K}}^{\mathrm{H}},\ \boldsymbol{C}_{\mathrm{nn}}^{(\mathrm{nc})} = \tilde{\boldsymbol{K}}\begin{bmatrix}\boldsymbol{C}_{\mathrm{nn}} & \boldsymbol{R}_{\mathrm{nn}} \\ \boldsymbol{R}_{\mathrm{nn}}^{*} & \boldsymbol{C}_{\mathrm{nn}}^{*}\end{bmatrix}\tilde{\boldsymbol{K}}^{\mathrm{H}}.$$

4.2. NC Unitary ESPRIT with Spatial Smoothing

We have shown in [15] and [16] that NC Standard ESPRIT and NC Unitary ESPRIT both using LS or SLS enjoy the same analytical performance in the high effective SNR. It was established that applying FBA to the augmented matrix $\boldsymbol{X}^{(\mathrm{nc})}$ does not improve the signal subspace estimate and that the real-valued transformation has no effect on the asymptotic performance in the high effective SNR. These properties still hold true if spatial smoothing is applied to both algorithms. It can be proven that the NC signal subspace for NC Standard ESPRIT and NC Unitary ESPRIT is modified in the same way.

5. SPECIAL CASE OF A SINGLE SOURCE

As the obtained closed-form MSE expressions for ESPRIT-type methods with spatial smoothing are deterministic, no Monte-Carlo simulations are required and the performance can be analyzed. However, the derived MSE expressions are formulated in terms of the

subspaces of the noise-free data matrix and thus, provide no explicit insights into the effect of physical parameters, e.g., the SNR, the number of sensors M, the sample size N, etc. Knowing how the performance scales with these system parameters can facilitate array design decisions or the choice of estimators. To establish a generally valid formulation is an intricate task, however, special cases can be considered. Inspired by [5], we consider a single source captured by a ULA with circularly symmetric white noise, i.e., $\boldsymbol{R}_{\mathrm{nn}} = \sigma_{\mathrm{n}}^2 \boldsymbol{I}_{MN}$ and $\boldsymbol{C}_{\mathrm{nn}} = \boldsymbol{0}_{MN}$. Due to space limitations, we only provide the final result. We have derived the MSE for Standard ESPRIT with spatial smoothing as

$$\mathrm{MSE} \approx \begin{cases} \frac{1}{\hat{\rho}} \cdot \frac{1}{(M-L)^2 L} & \text{if } L \leq M/2 \\ \frac{1}{\hat{\rho}} \cdot \frac{1}{(M-L)L^2} & \text{if} L > M/2, \end{cases} \tag{20}$$

where $\hat{\rho}$ represents the effective SNR $\hat{\rho} = N\hat{P}_{\mathrm{s}}/\sigma_{\mathrm{n}}^2$ and $\hat{P}_{\mathrm{s}}$ is the empirical source power given by $\hat{P}_{\mathrm{s}} = \|\boldsymbol{s}\|_2^2/N$. Here, the number of subarrays L is a design parameter that can be optimized. Therefore, minimizing the MSE expression with respect to L, we obtain $L_{\mathrm{opt}} = M/3$ for $L \leq M/2$ and $L_{\mathrm{opt}} = 2M/3$ for $L > M/2$, respectively, where we assume that M is a multiple of 3. For such M, the asymptotic efficiency can be explicitly computed as

$$\eta(L_{\mathrm{opt}}) \approx \lim_{\hat{\rho}\to\infty} \frac{\mathrm{CRB}}{\mathrm{MSE}} = \frac{8}{9} \cdot \frac{M^2}{M^2-1}, \tag{21}$$

where the single-source expression for the deterministic Cramér-Rao bound (CRB) is taken from [5]. Note that these results are in line with the ones previously found in [22] for harmonic retrieval in time series analysis. Interestingly, we obtain the same MSE and η for the spatially smoothed versions of Unitary ESPRIT as well as NC Standard and NC Unitary ESPRIT. Thus, in the single source case with spatial smoothing, no gain is achieved from FBA and non-circular sources.

6. SIMULATION RESULTS

In this section, we provide simulation results for the presented performance analysis of Standard and Unitary ESPRIT as well as NC Standard and NC Unitary ESPRIT with spatial smoothing. We compare the results found analytically to the empirical estimation errors obtained by averaging over Monte Carlo trials. A uniform linear array (ULA) with $M = 12$ isotropic elements spaced $\delta = \lambda/2$ apart is used. We assume that $d = 3$ sources with unit power that transmit real-valued symbols drawn from a Gaussian distribution impinge on the array with the spatial frequencies $\mu_1 = 0.25$, $\mu_2 = 0.5$, and $\mu_3 = 0.75$. Moreover, we assume white Gaussian circularly symmetric sensor noise. The curves show the total root mean squared error (RMSE) of the empirical simulations ("emp") for Standard and Unitary ESPRIT (SE/UE + SS) and NC Standard and NC Unitary ESPRIT (NC SE/UE + SS), and the square root of the analytical MSE expression denoted as ("ana"). We also compare our results to the deterministic CRBs for circular and strictly SO non-circular sources [24]. The results are obtained by averaging over 5000 runs.

Fig. 1 illustrates the RMSE versus the SNR, where $N = 5$, and the sources have a pair-wise correlation of $\rho = 0.9$. The rotation phases contained in $\boldsymbol{\Psi}$ are given by $\varphi_1 = 0$, $\varphi_2 = \pi/4$, and $\varphi_3 = \pi/2$. For L, we choose the obtained optimal value $L_{\mathrm{opt}} = M/3 = 4$. It can be seen that the analytical results agree well with the empirical estimation errors for high SNRs. Moreover, NC Standard and NC Unitary ESPRIT provide the lowest estimation errors and perform asymptotically identical at high SNRs.

In Fig. 2, we display the asymptotic efficiency of the considered ESPRIT-type algorithms for a single source versus the number of sensors M for $L_{\mathrm{opt}} = M/3$. The spatial frequency of the single source is drawn randomly as it has no impact on the MSE. The effective SNR is set to 46 dB, where $P_{\mathrm{s}} = 0$ dBW, $N = 4$, and $\sigma_{\mathrm{n}}^2 = 10^{-4}$. For comparison purposes, we include the case when no spatial smoothing is used, i.e., $L = 1$, and we obtain

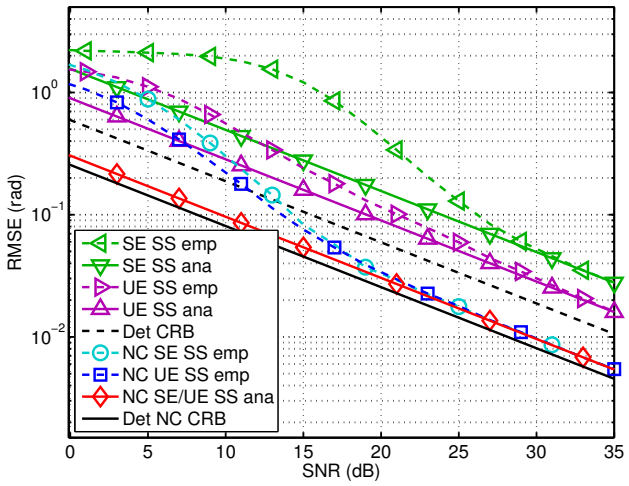

Fig. 1. Analytical and empirical RMSEs versus SNR for $M = 12$, $L = 4$, $N = 5$, and $d = 3$ correlated sources ($\rho = 0.9$) at $\mu_1 = 0.25$, $\mu_2 = 0.5$, $\mu_3 = 0.75$ with rotation phases $\varphi_1 = 0$, $\varphi_2 = \pi/4$, $\varphi_3 = \pi/2$.

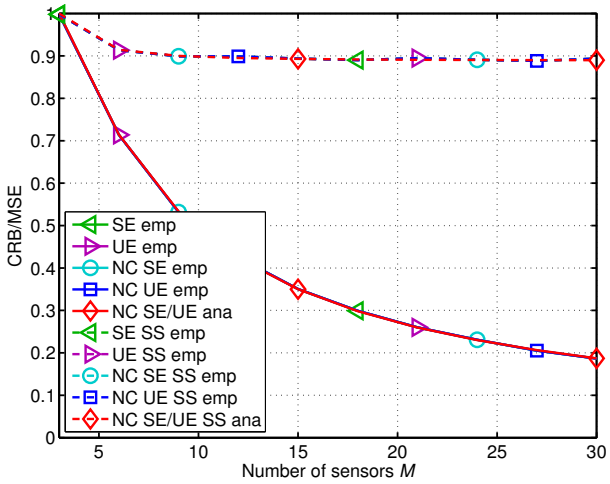

Fig. 2. Asymptotic efficiency versus M for a single source with an effective SNR of 46 dB ($P_{\mathrm{s}} = 0$ dBW, $N = 4$, $\sigma_{\mathrm{n}}^2 = 10^{-4}$).

$\eta(L = 1) = 6/M$. Fig. 2 shows that the efficiency of the algorithms with spatial smoothing is the same, approaching $8/9$, and considerably higher than that of those without spatial smoothing.

7. CONCLUSION

In this paper, we have developed a first-order analytical performance assessment of spatially smoothed versions of Standard and Unitary ESPRIT as well as NC Standard and NC Unitary ESPRIT. We have derived first-order expansions of the estimation errors, which are explicit in the noise perturbation and asymptotic in the high effective SNR. We have also derived MSE expressions that only assume the noise to be zero-mean with finite SO moments. We have shown that the NC Standard and NC Unitary ESPRIT versions perform asymptotically identical in the high effective SNR. However, NC Unitary ESPRIT should be preferred due to its better performance at low effective SNRs and its lower complexity. Moreover, we have considered the single source case, for which we have analytically derived the optimal number of subarrays L for spatial smoothing and shown that no improvements from forward-backward averaging and non-circular sources can be achieved in this case.

8. REFERENCES

[1] R. H. Roy and T. Kailath, "ESPRIT-estimation of signal parameters via rotational invariance techniques," *IEEE Transactions on Acoustics, Speech, and Signal Processing*, vol. 37, no. 7, pp. 984-995, July 1989.

[2] M. Haardt and J. A. Nossek, "Unitary ESPRIT: How to obtain increased estimation accuracy with a reduced computational burden," *IEEE Transactions on Signal Processing*, vol. 43, no. 5, pp. 1232-1242, May 1995.

[3] B. D. Rao and K. V. S. Hari, "Performance analysis of ESPRIT and TAM in determining the direction of arrival of plane waves in noise," *IEEE Transactions on Acoustics, Speech, and Signal Processing*, vol. 37, no. 12, pp. 1990-1995, Dec. 1989.

[4] F. Li, H. Liu, and R. J. Vaccaro, "Performance analysis for DOA estimation algorithms: Unification, simplifications, and observations," in *IEEE Transactions on Aerospace and Electronic Systems*, vol. 29, no. 4, pp. 1170-1184, Oct. 1993.

[5] F. Roemer and M. Haardt, "A framework for the analytical performance assessment of matrix and tensor-based ESPRIT-type algorithms," arXiv:1209.3253, Sept. 2012.

[6] F. Roemer, M. Haardt and G. Del Galdo, "Analytical performance assessment of multi-dimensional matrix- and tensor-based ESPRIT-type algorithms," *IEEE Transactions on Signal Processing*, Mar. 2014, accepted for publication.

[7] F. Roemer, H. Becker, and M. Haardt, "Analytical performance analysis for multi-dimensional Tensor-ESPRIT-type parameter estimation algorithms," in *Proc. IEEE Int. Conf. on Acoust., Speech, and Sig. Proc. (ICASSP)*, Dallas, TX, Mar. 2010.

[8] H. Abeida and J. P. Delmas, "MUSIC-like estimation of direction of arrival for noncircular sources," *IEEE Transactions on Signal Processing*, vol. 54, no. 7, pp. 2678-2690, July 2006.

[9] P. Chargé, Y. Wang, and J. Saillard, "A non-circular sources direction finding method using polynomial rooting," *Signal Processing*, vol. 81, no. 8, pp. 1765-1770, Aug. 2001.

[10] A. Zoubir, P. Chargé, and Y. Wang, "Non circular sources localization with ESPRIT," in *Proc. European Conference on Wireless Technology (ECWT 2003)*, Munich, Germany, Oct. 2003.

[11] M. Haardt and F. Roemer, "Enhancements of Unitary ESPRIT for non-circular sources," in *Proc. IEEE Int. Conf. on Acoust., Speech, and Sig. Proc. (ICASSP)*, Montreal, Canada, May 2004.

[12] P. J. Schreier and L. L. Scharf, *Statistical Signal Processing of Complex-Valued Data: The Theory of Improper and Noncircular Signals*, Cambridge, U.K.: Cambridge Univ. Press, 2010.

[13] H. Abeida and J. P. Delmas, "Statistical performance of MUSIC-like algorithms in resolving noncircular sources," *IEEE Transactions on Signal Processing*, vol. 56, no. 9, pp. 4317-4329, Sep. 2008.

[14] J. Steinwandt, F. Roemer, and M. Haardt, "Performance analysis of ESPRIT-type algorithms for non-circular sources," in *Proc. IEEE Int. Conf. on Acoust., Speech, and Sig. Proc. (ICASSP)*, Vancouver, Canada, May 2013.

[15] J. Steinwandt, F. Roemer, M. Haardt, and G. Del Galdo, "R-dimensional ESPRIT-type algorithms for strictly second-order non-circular sources and their performance analysis," arXiv:1402.2936, Feb. 2014.

[16] J. Steinwandt, F. Roemer, and M. Haardt, "Performance analysis of ESPRIT-type algorithms for strictly non-circular sources using structured least squares," in *Proc. Int. Workshop on Comp. Adv. in Multi-Sensor Adaptive Proc. (CAMSAP)*, Saint Martin, French Antilles, Dec. 2013.

[17] J. E. Evans, J. R. Johnson, and D. F. Sun, "Application of advanced signal processing techniques to angle of arrival estimation in ATC navigation and surveillance systems," MIT Lincoln Lab., Tech. Rep., Lexington, MA, 1982.

[18] T.-J. Shan, M. Wax, and T. Kailath, "On spatial smoothing for direction-of-arrival estimation of coherent signals," *IEEE Trans. Acoust., Speech, Signal Processing*, vol. ASSP–33, no. 4, pp. 806-811, Aug. 1985.

[19] A. Thakre, M. Haardt, and K. Giridhar, "Single snapshot spatial smoothing with improved effective array aperture," *IEEE Signal Processing Letters*, vol. 16, no. 6, pp. 505–508, June 2009.

[20] B. D. Rao and K. V. S. Hari, "Effect of spatial smoothing on the performance of MUSIC and minimum-norm method," *Proc. Inst. Elect. Eng.*, vol. 137, no.6, pp. 449-458, Dec. 1990.

[21] S. U. Pillai and B. H.Kwon, "Performance analysis of MUSIC-type high resolution estimators for direction finding in correlated and coherent scenes," *IEEE Trans. Acoust., Speech, Signal Processing*, vol. 37, no. 8, pp. 1176-1189, Aug. 1989.

[22] Y. Hua and T. K. Sarkar, "Matrix pencil method for estimating parameters of exponentially damped/undamped sinusoids in noise," *IEEE Trans. Signal Processing*, vol. 38, no. 5, pp. 814-824, May 1990.

[23] J. R. Magnus and H. Neudecker, *Matrix differential calculus with applications in statistics and econometrics*, John Wiley and Sons, 1995.

[24] F. Roemer and M. Haardt, "Deterministic Cramér-Rao bounds for strict sense non-circular sources," in *Proc. ITG/IEEE Workshop on Smart Antennas (WSA)*, Vienna, Austria, Feb. 2007.